Available online at www.sciencedirect.com
ScienceDirect
Quaternary Research 67 (2007) 115–127
QUATERNARY RESEARCH
www.elsevier.com/locate/yqres

Last glacial maximum equilibrium-line altitude and paleo-temperature reconstructions for the Cordillera de Mérida, Venezuelan Andes

Nathan D. Stansell [a,*], Pratigya J. Polissar [b], Mark B. Abbott [a]

[a] *Department of Geology and Planetary Science, University of Pittsburgh, Pittsburgh, PA 15260, USA*
[b] *Department of Geosciences, The Pennsylvania State University, University Park, PA 16802, USA*

Received 1 July 2005
Available online 5 October 2006

Abstract

The pattern and magnitude of glacier equilibrium-line altitude (ELA) lowerings in the tropics during the last glacial maximum (LGM) are topics of current debate. In the northern tropics, paleo-ELA data are particularly limited, inhibiting the ability to make regional and large-scale paleoclimatic inferences. To improve these records, nine paleo-glaciers in the Venezuelan Andes were reconstructed based on field observations, aerial photographs, satellite imagery and high-resolution digital topographic data. Paleo-glacier equilibrium-line altitudes (ELAs) were estimated using the accumulation-area ratio (AAR) and the area-altitude balance ratio (AABR) methods. During the local LGM in Venezuela (~22,750 to 19,960 cal yr BP), ELAs were ~850 to 1420 m lower than present. Local LGM temperatures were are at least 8.8±2°C cooler than today based on a combined energy and mass-balance equation to account for an ELA lowering. This is greater than estimates using an atmospheric lapse rate calculation, which yields a value of 6.4±1°C cooler. The paleo-glacial data from the Venezuelan Andes support other published records that indicate the northern tropics experienced a greater ELA lowering and possibly a greater cooling than the Southern Hemisphere tropics during the LGM.

Keywords: Northern hemisphere tropics; Climate change; Tropical glacier mass-balance

Introduction

The CLIMAP project reconstruction of tropical sea surface temperatures (SSTs) has led to extensive debate about the degree of atmospheric cooling that took place in the tropics during the last glacial maximum (LGM). CLIMAP (CLIMAP, 1976, 1981) proposed that tropical SSTs were 1° to 3°C cooler during the LGM. However, glacial-geological evidence suggests that higher elevations in the tropics experienced much greater cooling (e.g. Porter, 2001). New proxies and re-evaluation of the CLIMAP data has resolved some of the discrepancy (Mix et al., 1999). However, this has not resolved the fundamental differences between LGM estimates of SST and high-altitude tropical temperatures. Understanding this discrepancy has implications for climate modeling, particularly for determining the vertical structure of the troposphere and water vapor feedbacks during the LGM (Betts and Ridgeway, 1992; Broecker, 1997).

There is considerable controversy regarding the interpretation of changes in tropical glacial extent during the LGM. These changes are commonly summarized by the fluctuations in the equilibrium-line altitude (ELA, the dividing line between a glacier's accumulation and ablation areas). It has recently been argued that reconstructed tropical LGM ELA lowerings of 900 m or more may be anomalously large due to local enhancing factors such as shading by valley walls, debris cover, or orographically controlled precipitation patterns and should therefore be used with caution for paleoclimatic inferences (Smith et al., 2005). This is contrary to Porter's (2001) detailed synthesis, which shows evidence that during the LGM a large number of tropical ELA values were 800 to 1000 m lower than today. Recent reports indicate that ELAs during the LGM were up to ~1500 m lower in the northern tropics (Mark et al., 2005). However, the data used by Mark et al. (2005) for Venezuela

* Corresponding author. Fax: +1 412 624 3914.
E-mail address: nas12@pitt.edu (N.D. Stansell).

0033-5894/$ - see front matter © 2006 University of Washington. All rights reserved.
doi:10.1016/j.yqres.2006.07.005

were based on poorly defined glacial-geologic data and paleo-ELA values. Here, LGM ELA values for nine individual paleoglaciers in the Venezuelan Andes were investigated in order to better understand the limits of tropical LGM glaciation and to reduce ambiguity in paleo-ELA values caused by local factors. The magnitude of high-elevation tropical cooling was then investigated by reconstructing temperature change in the Venezuelan Andes during the LGM. The associated paleotemperature values were determined using a combined energy and mass-balance equation, which provides a more comprehensive estimate of cooling than commonly used atmospheric lapse rate calculations.

Background

Timing of the LGM

The globally averaged LGM is centered at ~21,000 cal yr BP; however, the timing of the LGM in specific regions has been found to lead or lag the CLIMAP global average by up to several thousand years (e.g., Mann and Hamilton, 1995; Lowell et al., 1995; Denton et al., 1999; Seltzer et al., 2002; Smith et al., 2005). In the Venezuelan Andes, the local LGM occurred between 22,750 and 19,960 cal yr BP (Schubert and Rinaldi, 1987). During this period, glaciers covered ~200 km^2 of surface area and extended to elevations as low as 2900 m (Schubert and Clapperton, 1990).

Glacier extent and climatic change

The relationship between glacier coverage and climate change is a challenging issue in paleoclimatology. Using the ELA as a measure of glacier extent, it is possible to model the response of modern glaciers to climate change (Hastenrath, 1984, 1989; Ames and Francou, 1995; Francou et al., 1995; Kaser, 1995; Kaser and Noggler, 1996; Oerlemans, 2001; Kaser and Osmaston, 2002). However, the climate change associated with alpine glaciations during the LGM is difficult to gage because the associated meteorological conditions are not well constrained. Therefore, glacial geologists commonly rely on simple atmospheric lapse rate calculations to estimate the temperature change responsible for an ELA lowering. These calculations do not accurately represent the energy exchange at the glacier surface and ignore the effects of changes in accumulation (Seltzer, 1994). As an alternative, models that combine energy and mass-balance equations may be used in order to reconstruct the temperature change associated with an ELA lowering (Kuhn, 1989; Seltzer, 1994). In addition to the atmospheric temperature lapse rate, these models take into consideration the effects of vertical gradients in precipitation and humidity, and allow for secular changes in accumulation and solar radiation.

Differences between tropical and temperate glaciers

The mass-balance profiles of glaciers are controlled by rates of accumulation and ablation along the surface of a glacier and vary depending upon the climate regime. For instance, glaciers in the tropics are differentiated from temperate ones because they are affected by the annual migration of the Intertropical Convergence Zone (ITCZ) and experience greater diurnal than annual temperature variation (Kaser, 1995; Kaser and Noggler, 1996). Further, inner tropical glaciers receive precipitation year-round and are most sensitive to changes in temperature (Kaser, 2001). Outer tropical glaciers experience nearly constant temperature year-round but precipitation is strongly seasonal. Therefore, outer tropical glaciers have an annual mass-balance that is seasonal and sensitive to variations in both precipitation and temperature (Kaser and Georges, 1999).

The climate of the Venezuelan Andes is intermediate between the inner and the outer tropics because this region experiences seasonal precipitation combined with high humidity throughout the year (Azocar and Monasterio, 1980). These conditions play an important role in the mass-balance process because humid air inhibits latent heat loss through sublimation and promotes melting. Melting is a faster and more efficient ablation process than sublimation because it requires less energy. High ablation rates reduce the overall glacier surface area below the equilibrium-line that is needed to balance accumulation. As a result, a substantial part of a humid tropical glacier's surface area is maintained in the accumulation zone and the equilibrium-line is situated near the base of the glacier (Kaser and Osmaston, 2002).

Study area

This study focuses on the Cordillera de Mérida of the Venezuelan Andes, located between 8.5 and 9°N at elevations above 2900 m (Fig. 1). Three geographic sub-regions were studied that have different aspects and span an orographic precipitation gradient. From southeast to northwest, these regions are: (1) the southern Sierra de Santo Domingo, (2) the northern Sierra de Santo Domingo and (3) the Paramo de Piedras Blancas.

Modern climate

Moisture in northern South America is primarily derived from Atlantic Ocean evaporation. Easterly trade winds transport this moisture into the interior of the continent. In the Mérida Andes, circulation patterns and steep topography combine to form strong east-to-west precipitation and cloud-cover gradients. Diurnal patterns of circulation and cloudiness have been shown to contribute to an asymmetry in precipitation and glaciation for other tropical South American and African regions (e.g. Hastenrath, 1985; Mölg et al., 2003). This diurnal pattern is observed in the Mérida Andes, where cloud cover is minimal during the morning hours and increases throughout the day. In the Sierra de Santo Domingo, the east-facing slopes receive high solar radiation, whereas afternoon cloudiness reduces the amount of radiation reaching the west-facing slopes. In the Paramo de Piedras Blancas, conditions are drier than in the Santo Domingo region and cloud cover is minimal throughout the majority of the day.

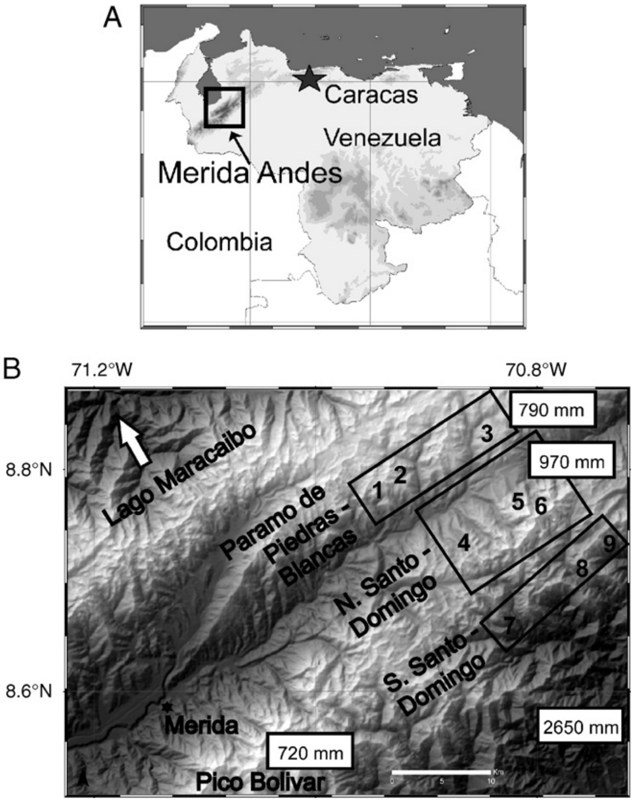

Figure 1. (A) Location map of the Cordillera de Mérida, Venezuela. (B) Average annual precipitation (mm/yr) for select areas, shaded relief image of the Cordillera de Mérida and index map of reconstructed glaciers: (1) Las Viraviras, (2) Cerro Los Pantanos, (3) El Balcon, (4) Michurao, (5) Mucubají, (6) Negra, (7) Llano del Trigo, (8) Filo Los Pantanos, (9) Granates. Precipitation values (white boxes) are greatest on southeast-facing slopes in the study area and decrease on northeast-facing slopes. The black boxes represent the three geographic sub-regions used in this study.

The climate of the Mérida Andes is cold and humid throughout the year (Azocar and Monasterio, 1980). Precipitation is controlled by the position and intensity of the ITCZ, which is linked to the seasonal cycle of solar declination. Precipitation patterns have a bimodal annual distribution at lower elevations near Mérida (1498 m), with peaks in May–June and September–November and a minimum in July–August (Bradley et al., 1991). A shift to a unimodal precipitation regime occurs at elevations above Mérida, where the wet season occurs from April–November and peaks in June (Pulwarty et al., 1998).

The regional pattern of precipitation can be determined from the available station data (Table 1). The closest station to the southern Sierra de Santo Domingo has a similar aspect and receives ~2650 mm/yr of precipitation. The elevation (550 m) of this station is lower than the study area (3000 m) where precipitation is probably lower. Adjusting for elevation using the precipitation gradient from Pulwarty et al. (1998), the precipitation for the southern Sierra de Santo Domingo region is probably ~1600 mm/yr. The Mucubají precipitation data record ~970 mm/yr and represent the northern Sierra de Santo Domingo. Pico Aguila is representative of the Paramo de Piedras Blancas and records an average precipitation of ~790 mm/yr. The data for Pico Aguila were adapted from Monasterio and Reyes (1980) and Monasterio (1986) and must be evaluated carefully because collection times and techniques were not specified. East of Piedras Blancas, station data recorded 1190 mm/yr of precipitation for the Paramo de La Culata (Schubert and Valastro, 1974), but monthly values are not available.

Temperature in the Cordillera de Mérida is typical of the low latitudes and shows little seasonal variability but a substantial diurnal freeze–thaw cycle. Daily temperatures vary as much as 20°C (Schubert and Clapperton, 1990) and greatly exceed the total annual variation. National Center for Environmental Prediction (NCEP) data indicate that the free-atmosphere lapse rate is ~0.55°C/100 m for this region of the Andes (Kalnay et al., 1996). Environmental lapse rates based on station data from the Mérida Andes range from 0.4° to 0.7°C/100 m, with an average of 0.6°C/100 m (Salgado-Labouriau, 1979; Bradley et al., 1991).

Modern and past glaciation of the Venezuelan Andes

Glaciers in Venezuela are currently restricted to Picos Bolivar (5002 m), Humboldt (4942 m) and Bonpland (4839 m). These cirque glaciers cover less than ~2 km^2 and extend down to elevations of ~4450 m. Glaciers at these locations have been continuously retreating during historical times (Schubert, 1984, 1998) and are currently not in equilibrium with the modern climate.

There is abundant evidence for more extensive glacier coverage in the Cordillera de Mérida during the LGM and it is estimated that glaciers covered approximately 200 km^2 (Schubert and Clapperton, 1990). Schubert and Rinaldi (1987) concluded that the local LGM for Venezuela occurred

Table 1
Precipitation data from the Cordillera de Mérida, Venezuela

Station	Lat (°N)	Lon (°W)	Alt. (m)	Average monthly precipitation (mm)												
				Jan	Feb	Mar	Apr	May	Jun	Jul	Aug	Sep	Oct	Nov	Dec	Year
Barintas[1]	8.80	70.80	550	41	49	83	247	332	347	331	337	310	316	182	73	2647
Mucubají[2,3]	8.80	70.83	3650	19	15	26	104	101	153	149	124	110	95	51	21	969
P. Aguila[3]	8.87	70.80	4118	18	17	29	75	101	105	105	97	95	95	36	17	790
Merida[1]	8.60	71.18	1498	47	48	64	167	243	162	119	142	194	263	201	86	1737
P. Espejo[4]	8.58	71.17	4765	15	17	38	85	97	80	54	75	89	81	56	30	717

Source: (1) Global Historical Climatology Network, (2) Bradley et al. (1991), (3) Monasterio and Reyes (1980), (4) Pulwarty et al. (1998).

https://doi.org/10.1016/j.yqres.2006.07.005 Published online by Cambridge University Press

between ~22,750 and 19,960 cal yr BP based on radiocarbon dating of interbedded peat deposits in a 30-m-thick glacio-fluvial sequence in the northern Santo Domingo region. The associated glaciation produced extensive glacial-geomorphic features, including pronounced moraine systems (Schubert, 1974).

Previous research has identified principal moraines at two levels: a lower level between 2600 and 2800 m and an upper level between 2900/3000 and 3500 m (Schubert, 1970, 1974, 1992; Giegengack and Grauch, 1973; Schubert and Valastro, 1974; Schubert and Rinaldi, 1987; Schubert and Clapperton, 1990). The lower level is characterized by weathered till covered by abundant vegetation, whereas the upper level is characterized by fresh, well-preserved till forming prominent ridges. The lower levels appear to date to ~81,000 yr (Mahaney et al., 2000). Schubert (1974) concluded that the upper level represents the last major local glacial advance, which he termed the late Pleistocene Mérida glaciation. Age control for LGM deposits is best constrained for the N. Santo Domingo region and glaciers presented in this report are assumed to be contemporaneous to the LGM based on Schubert's (1974, 1987) investigations.

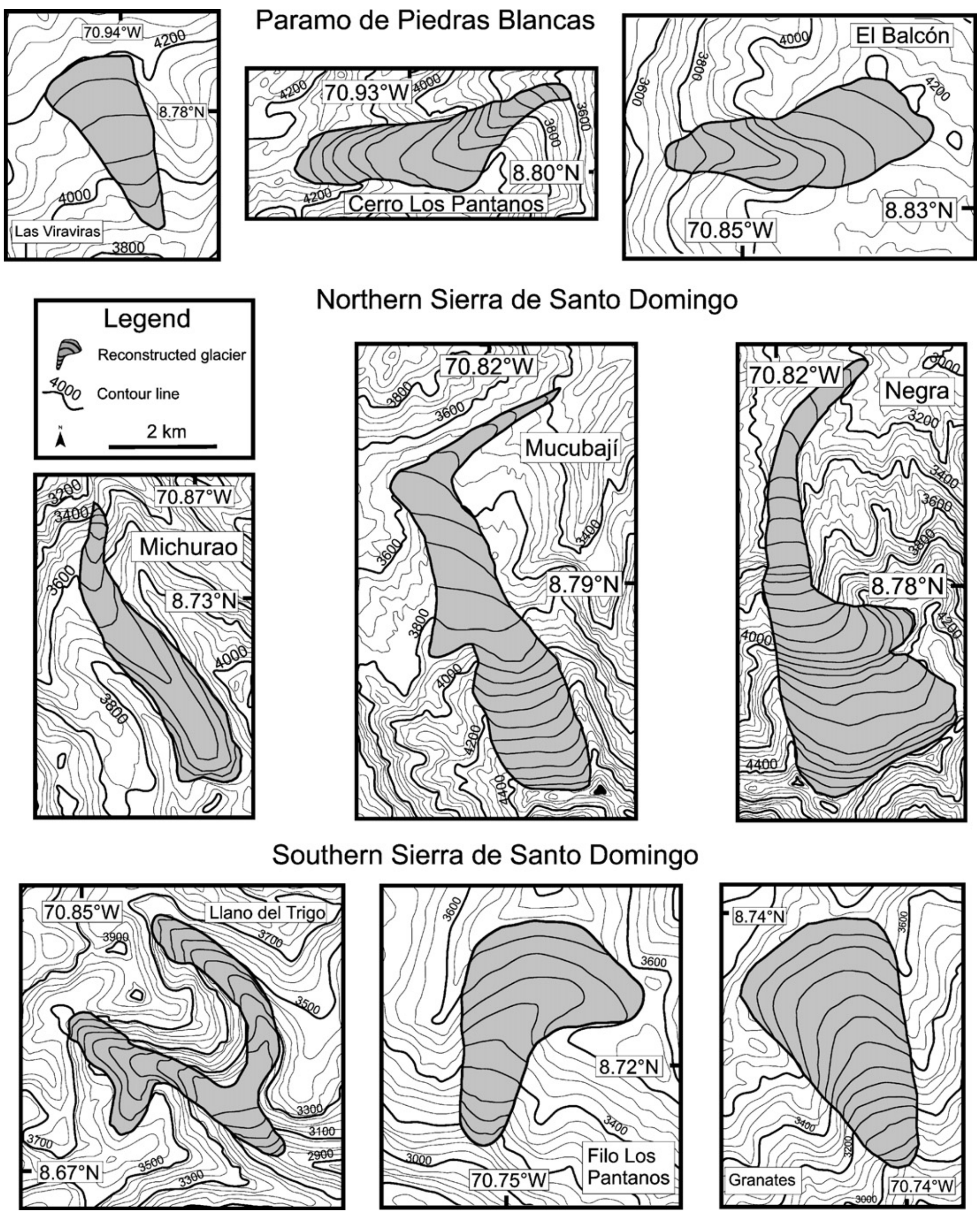

Figure 2. Venezuela LGM reconstructed glaciers. The base map was contoured based on published maps at a 40-m interval. Paleo-glacier surface contours were based on SRTM data at a 50-m interval. Paleo-glaciers were grouped by geographic sub-region, separated by aspect and precipitation amounts. The southern Sierra de Santo Domingo receives the greatest precipitation in the study site whereas the Paramo de Piedras Blancas receives the least.

https://doi.org/10.1016/j.yqres.2006.07.005 Published online by Cambridge University Press

Methods

Mapping and surface reconstruction of paleo-glaciers

Schubert (1987) mapped and identified late Pleistocene glacial features in the Mérida Andes using photographs from the Cartografía Nacional aerial photograph mission of 1952. These maps were digitized on a smaller scale for this project. Because aerial photographs are susceptible to planimetric distortions and are limited in spatial coverage, Advanced Spaceborne Thermal Emission and Reflection Radiometer (ASTER) data were also used for digital mapping. Each ASTER scene can be used to produce false-color composite images with ~15-m resolution over a broad spatial area.

Spatial information and elevation data used for contouring were derived from Shuttle Radar Topography Mission (SRTM) data. These data were processed by the SRTM ground data processing system at the Jet Propulsion Laboratory (JPL) and were post-processed by the National Imagery and Mapping Agency (NIMA). Elevation values are presented in meters and referenced to the WGS84 geoid. Digital elevation models (DEMs) with 3 arc-second resolution (~90 m) for South America have been derived from SRTM data and were downloaded from the JPL. DEMs were imported into ArcGIS® 9.0 software for spatial analyses.

Paleo-glaciers were reconstructed in valleys with straightforward geometries and well preserved paleo-glacial landforms to ensure accurate mapping. In each sub-region, three glaciers were reconstructed to increase the signal/noise ratio. This sampling scheme was used in an attempt to minimize the importance of local variables, such as wind speed, precipitation and cloudiness, and maximize the signal of regional parameters by reconstructing multiple glaciers. In addition, reconstructing glaciers from different regions allows for characterization of the regional paleo-ELA gradient and comparison with modern observations. A transect of paleo-glacial valleys was studied, from the wet southeast-facing slope of the Sierra de Santo Domingo to the drier Paramo de Piedras Blancas.

Table 2
Spatial data and LGM ELA values for the Sierra Nevada de Mérida, Venezuela

Paleo-glacier name	Location (DD)	Headwall Contour (m)	Terminus Contour (m)	τ_b: avg. shear stress (kPa)	Balance Ratio (BR)	Calculated LGM ELA (m asl)	Accumulation–Area Ratio (AAR)	Modern ELA (minimum estimate)	Modern ELA (maximum estimate[2])	ELA lowering (Δ ELA) min	ELA lowering (Δ ELA) max
Paramo de Piedras Blancas [a, b]											
Las Viraviras	8.78°N	4200	3900	126	5	4030	0.77	4880	5040	−850	−1010
	70.94°W				10	4010	0.82	4880	5040	−870	−1030
					15	4000	0.84	4880	5040	−880	−1040
Cerro Los	8.80°N	4300	3600	103	5	3900	0.76	4880	5040	−980	−1140
Pantanos	70.93°W				10	3855	0.83	4880	5040	−1025	−1185
					15	3830	0.85	4880	5040	−1050	−1210
El Balcón	8.83°N	4200	3700	92	5	3930	0.74	4880	5040	−950	−1110
	70.85°W				10	3890	0.83	4880	5040	−990	−1150
					15	3880	0.84	4880	5040	−1000	−1160
Average						3930				−960	−1120
Northern Sierra de Santo Domingo [b, c]											
Mucubají	8.79°N	4550	3350	97	5	3710	0.66	4670	4950	−960	−1240
	70.82°W				10	3670	0.73	4625	4950	−955	−1280
					15	3640	0.78	4610	4950	−970	−1310
Negra	8.78°N	4500	3200	83	5	3725	0.77	4620	4950	−895	−1225
	70.82°W				10	3620	0.81	4625	4950	−1005	−1330
					15	3560	0.85	4615	4950	−1055	−1390
Michurao	8.73°N	4150	3250	83	5	3650	0.75	4610	4950	−960	−1300
	70.87°W				10	3610	0.84	4610	4950	−1000	−1340
					15	3590	0.87	4600	4950	−1010	−1360
Average						3640				−980	−1310
Southern Sierra de Santo Domingo [a,b]											
Filo Los	8.70°N	3700	3200	123	5	3505	0.68	4470	4630	−965	−1125
Pantanos	70.75°W				10	3460	0.76	4470	4630	−1010	−1170
					15	3435	0.82	4470	4630	−1035	−1195
Granates	8.73°N	3650	3000	143	5	3300	0.73	4470	4630	−1170	−1330
	70.73°W				10	3260	0.78	4470	4630	−1210	−1370
					15	3230	0.82	4470	4630	−1240	−1400
Llano del	8.67°N	3650	2950	105	5	3265	0.73	4470	4630	−1205	−1365
Trigo	70.85°W				10	3230	0.81	4470	4630	−1240	−1400
					15	3210	0.86	4470	4630	−1260	−1420
Average						3320				−1150	−1310

[a] Modern ELA minumum values calculated using a freezing height of 4700 m.
[b] Modern ELA maximum values calculated using a freezing height of 4860 m.
[c] Minimum ELA values for the northern Sierra de Santo Domingo were estimated using the existing glaciers on Pico Bolivar (Polissar, 2005).

https://doi.org/10.1016/j.yqres.2006.07.005 Published online by Cambridge University Press

Using a composite of aerial photographs and the ASTER scene, nine paleo-glaciers from three mountain slopes were mapped (Fig. 2). Glacier surfaces were contoured at a 50-m interval and the spacing was constrained by calculating the basal shear stress (τ_b), which results from the slope of the glacier and bedrock surfaces (Seltzer, 1992):

$$\tau_b = \rho gtf(\Delta h/\Delta x), \quad (1)$$

where ρ is the density of ice (0.93 g/cm^3), g is the acceleration due to gravity (9.80 m/s^2), t is the centerline thickness (m), f is a shape factor ($f=A/Pt$, where A is the area and P is the wetted perimeter of a given cross-section of the glacier) and $\Delta h/\Delta x$ is the slope of the ice surface. Calculated shear stress values (Table 2) should approximate those of modern glaciers, which tend to be between 50 and 150 kPa (Paterson, 1981). Horizontal spacing of contours was adjusted if the shear stress value fell outside of this range.

Surface contours were drawn convex near the terminus, straight at mid-elevations and concave near the headwall. A separate polygon was created for each contour range, delimiting that section of the glacier using the GIS software. A grid surface was created for each polygon, using the spatial data stored in the DEM. The total area between each pair of successive contours was then determined. A hypsometric plot was generated using the calculated surface areas for each separate polygon (Fig. 3).

Paleo-ELA reconstructions

The ELA is a statistical concept representing the dividing line between the accumulation and ablation zones. Various methods for reconstructing paleo-ELAs have been critically reviewed (Meirding, 1982; Benn and Evans, 1998; Porter, 2001; Kaser and Osmaston, 2002; Osmaston, 2005). The more comprehensive reconstruction methods take into consideration the size, shape and distribution of total ice surface area versus elevation. For example, the accumulation area ratio (AAR) method assumes that the accumulation area of a glacier occupies a fixed proportion of a glacier's total surface area. The ELA is then determined by applying an estimated AAR value to a hypsometric plot. Temperate glaciers have an average AAR of approximately 0.65 and this value has been commonly applied to tropical glacier hypsometries (e.g. Porter, 2001). Likewise, Klein et al. (1999) used a tropical AAR average of 0.67 in their study based on work by Jordan (1991). AAR values should be higher in the humid tropics than the mid-latitudes because melting occurs throughout the year and the surface area in the ablation zone required to compensate for mass accumulation is less than that of temperate glaciers (Kaser and Osmaston, 2002). It has been observed that AAR values of modern humid tropical glaciers are as high as 0.8 (Kaser and Osmaston, 2002; Mölg et al., 2003).

The mass-balance gradient of a glacier is a measure of the rates of accumulation and ablation as a function of elevation. The AAR method assumes that the rates of accumulation and ablation are fixed with altitude and does not consider the

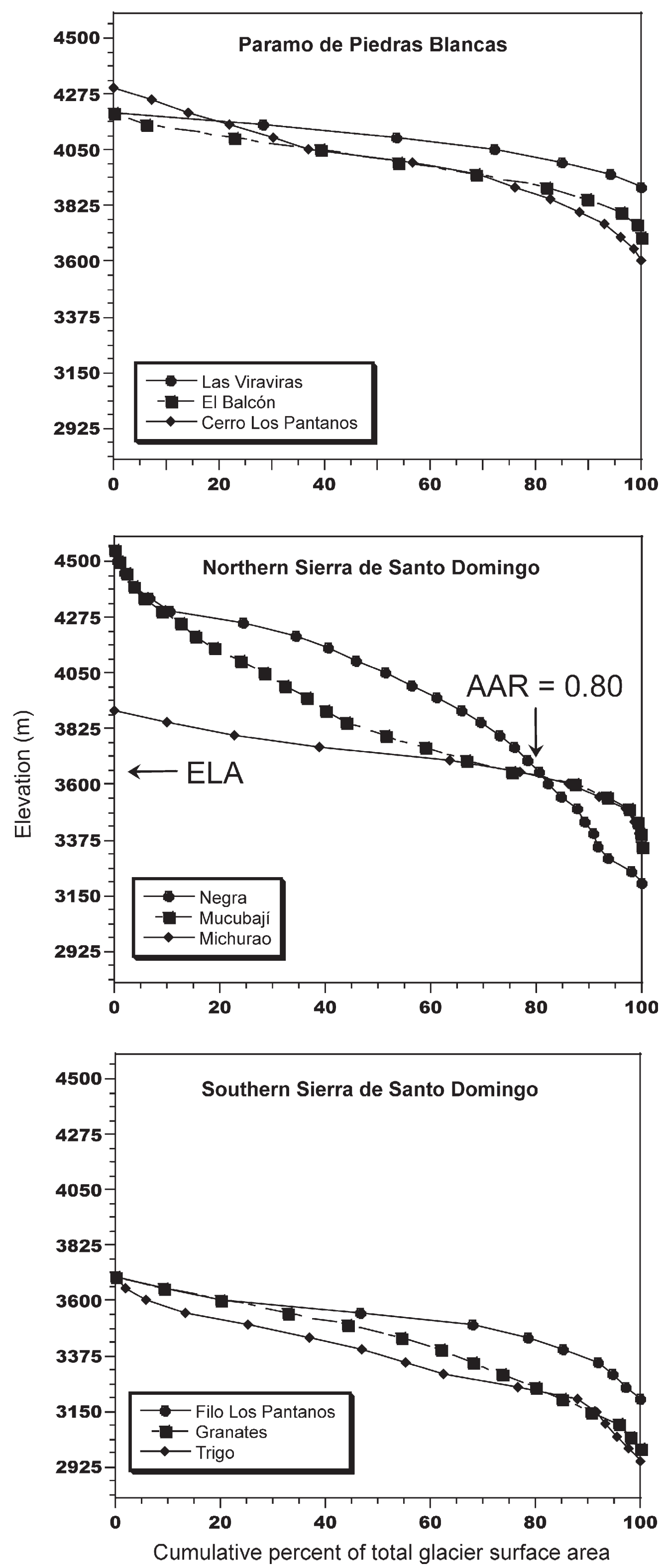

Figure 3. Hypsometric plots of the nine Venezuela LGM glaciers used in this study. The paleo-ELAs were estimated by applying an AAR value to the plot and determining the corresponding elevation. The three separate boxes represent the geographic sub-regions used in the study. The Balance Ratio method was also applied to these data (Table 2). The paleo-ELA values for the northern Sierra de Santo Domingo were used for paleo-temperature estimates (Eq. (3)).

https://doi.org/10.1016/j.yqres.2006.07.005 Published online by Cambridge University Press

vertical mass-balance profile of a glacier. As an alternative, the area–altitude–balance ratio (AABR) method takes into consideration both the hypsometry of the glacier and the shape of the mass-balance curve (Furbish and Andrews, 1984; Benn and Evans, 1998; Osmaston, 2005). The balance ratio (BR) is defined as the ratio of the mass-balance gradients of the ablation and accumulation zones. As with an AAR value, the BR values are higher in the tropics than in temperate regions because of the relatively high rates of ablation. Tropical glaciers typically have BR values of 2 to 5, but this value can be as high as 25 (Benn and Evans, 1998). ELAs were estimated with the AABR method using a spreadsheet developed by Osmaston (2005).

In this study both the AAR and AABR methods were used to determine paleo-ELAs. The proper BR and AAR values are not known for the Venezuelan Andes because the mass-balance profiles of the existing modern glaciers have not been directly observed. Therefore, we used both methods with a range in AAR and BR values (Table 2). The AABR method with a BR value of 5 yields an ELA that closely matches the AAR method with a value of 0.73 for the northern Sierra de Santo Domingo region. Given the strongly seasonal precipitation and continuously high humidity in this region, these should be considered minimum estimates. More appropriate AAR values are likely around 0.80, which corresponds to a BR of ~10.

As a final note, it is important to consider the effects of lower sea level during the LGM on glacier ELAs. LGM sea level was 120 m lower than present (Fairbanks, 1989). As a result, the global atmosphere may have descended by a comparable amount and paleo-ELA values may need to be compensated (Porter, 2001). However, convincing arguments have been made that the transfer of water from the oceans to land displaced enough atmospheric mass to compensate for the lower sea level (Osmaston, 2006), and thus both modern and LGM ELAs should be referenced to modern sea level. Here all elevations are reported above modern sea level and calculated LGM ELA lowerings are not corrected for lower sea level.

Determining modern ELAs

The existing glacier on the north-facing slope of Pico Bolivar was used to calculate the modern ELA of the northern Sierra de Santo Domingo, because both regions have similar aspects and seasonal precipitation patterns. The existing glaciers were observed in the field and mapped by Schubert (1972). The modern ELAs were estimated using the AAR method applied to a hypsometric plot generated by Polissar (2005) and the results are presented in Table 2. During the LGM, glaciers on Pico Bolivar were part of a large ice cap with a complex geometry and are therefore not included in the paleo-glacier reconstructions presented in this paper.

The Pico Bolivar glaciers provide a minimum estimate of a modern ELA for the northern Santo Domingo because they are out of equilibrium with today's climate and are retreating rapidly. Schubert (1992) documented a rise in the regional snowline from ~4100 m in AD 1885 to above 4700 m during the 1970's. National Centers for Environmental Prediction (NCEP) reanalysis data show that the modern regional freezing level is ~4860 m (Kalnay et al., 1996). Alternative maximum modern ELA estimates considered the NCEP freezing height (Table 2).

The ELA can be roughly approximated in regions where modern glaciers do not exist if the freezing height is known by using the following equation (Greene et al., 2002):

$$\mathrm{ELA} = 537 + 1.01\mathrm{FH} - 0.51\mathrm{P}, \tag{2}$$

where FH is the estimated annual freezing height (m a.s.l.), and P is the annual precipitation (mm). Modern ELAs for the Paramo de Piedras Blancas and the southern Sierra de Santo Domingo were estimated using Eq. (2). Minimum and maximum values were estimated using freezing heights of 4700 and 4860 m, respectively. It should be noted that this equation represents a statistical average for tropical glaciers and needs to be evaluated carefully when applied to individual glaciers.

Paleo-temperature reconstruction

Seltzer (1992) modified Kuhn's (1989) equation to calculate the temperature change (ΔT) responsible for a ΔELA:

$$\Delta T = \frac{L_\mathrm{m}}{A_\mathrm{H}}\left(\frac{\partial P}{\partial z}\Delta\mathrm{ELA} + \Delta P\right) + \frac{1}{A_\mathrm{H}}\left[\frac{L_\mathrm{m}}{L_\mathrm{s}} - 1\right]\left[A_\mathrm{s}\frac{\partial p_\mathrm{va}}{\partial z}\Delta\mathrm{ELA}\right] - \frac{\partial T}{\partial z}\Delta\mathrm{ELA}, \tag{3}$$

where L_m is the latent heat of melting, L_s is the latent heat of sublimation, A_H is the transfer coefficient for sensible heat, A_S is the transfer coefficient for latent heat, $\partial P/\partial z$ is the vertical precipitation gradient, $\partial p_\mathrm{va}/\partial z$ is the vertical gradient in atmospheric absolute humidity, $\partial \mathrm{Ta}/\partial z$ is the atmospheric lapse rate, ΔP is the change is precipitation and ΔELA is the change in ELA (refer to Tables 3 and 4 for the corresponding values). The first term of this equation reflects the contribution from changes in precipitation over time and precipitation change as a function of elevation. The second term reflects how an ELA-inferred temperature lowering is affected by a vertical change in atmospheric humidity (Seltzer, 1992). The final term incorporates the temperature change resulting from the atmospheric temperature lapse rate. Values for precipitation were derived from modern station data. Values of ±50% of the modern mean were also used to model the possible effects of changes in precipitation during the LGM. The precipitation gradient was estimated using the regional maximum and minimum values from Pulwarty et al. (1998). The atmospheric humidity gradient was estimated using the modern annual mean calculated from NCEP data and a range in LGM humidity gradient values were estimated by taking ±50% of the modern mean. The transfer coefficients were based on values of resistance to sensible and latent heat transfer from Kaser and Osmaston (2002).

https://doi.org/10.1016/j.yqres.2006.07.005 Published online by Cambridge University Press

Table 3
Venezuela LGM temperature values as a function of changes in the atmospheric lapse rate and precipitation using the Kuhn (1989) equation

ΔELA = −980 m		
Lapse rate °C/100 m	Δ*P* mm/yr	ΔT °C
	+500	−7.47
0.55	0	−7.83
	−500	−8.19
	+500	−8.45
0.65	0	−8.81
	−500	−9.17
	+500	−9.42
0.75	0	−9.79
	−500	−10.15

Determining an appropriate LGM atmospheric lapse rate requires careful consideration because these values introduce a large potential error in the paleo-temperature calculation. The average modern tropical lapse rate is 0.6°C/100 m (Porter, 2001). The published modern lapse rates for Venezuela range from 0.54 to 0.63°C/100 m (Salgado-Labouriau, 1979; Bradley et al., 1991; Kalnay et al., 1996). In addition, atmospheric conditions during the LGM in the Venezuelan Andes were probably more arid than today (Bradbury et al., 1981; Bradley et al., 1985; Weingarten et al., 1991; Salgado-Labouriau et al., 1992), which may have resulted in steeper atmospheric lapse rates. Using steeper lapse rates is not necessarily justified, however, because it has been documented that even dry tropical locations tend to approach the maximum of the saturated adiabatic lapse rate (Rind and Peteet, 1985). A minimum estimate for an LGM atmospheric lapse rate in the Venezuelan Andes is probably close to the modern minimum of 0.55°C/100 m. The maximum plausible LGM tropical atmospheric lapse rate is probably ∼0.75°C/100 m (Kaser and Osmaston, 2002).

Results

Last glacial maximum ELA values

The combined results of the AABR and AAR methods were used to estimate the LGM ELA values. Minimum ELAs were estimated using AAR and the corresponding BR values that approximate reported tropical averages (e.g. Klein et al., 1999; Porter, 2001). Conversely, maximum ELAs were estimated using larger AAR and BR values that are conceptually more plausible for this region based on reports from existing tropical glaciers (Benn and Evans, 1998; Kaser and Osmaston, 2002; Mölg et al., 2003). Higher BR and AAR values also provided the least variance in the estimated ELA values in this study area, supporting the contention that they are more appropriate for this region. Results from the Paramo de Piedras Blancas indicate that LGM ELA values were between ∼4030 and 3830 m. In the northern Sierra de Santo Domingo, LGM ELA values were between ∼3725 and 3560 m. The southern Sierra de Santo Domingo LGM ELA values were between ∼3505 and 3210 m (Table 2). The average ELA values indicate that the LGM ELA gradient was ∼600 m across the 25 km study site (Fig. 4).

The LGM ELA lowering (ΔELA) can be estimated by comparing the modern glaciers on Pico Bolivar to the reconstructed LGM glaciers in the northern Sierra de Santo Domingo. The range of modern ELA values for the northern-most glacier on Pico Bolivar was estimated using the same range of AAR values for the northern Sierra de Santo Domingo paleo-glaciers. The average LGM ELA value for the northern Sierra de Santo Domingo is ∼3640 m, which yields an average ΔELA of −980 m.

Last glacial maximum temperature reconstruction

The most reliable LGM ΔELA values are from the northern Sierra de Santo Domingo region because modern glaciers exist for comparison and age of the glacial deposit is constrained. Therefore a paleo-temperature calculation was only applied to the N. Santo Domingo region. The applied temperature equation requires an ∼8.8°C local LGM cooling to explain a ΔELA of −980 m using modern values for precipitation. Increasing or decreasing precipitation by up to 50% relative to modern values only results in a ±0.5°C change in the overall temperature calculation.

A sensitivity analysis of the effects of each variable used in Eq. (3) was conducted to better constrain the uncertainty in the calculated temperature change (Table 4). For example, the uncertainty in the atmospheric lapse rate value provides the

Table 4
Error analysis in the estimation of ΔT for the LGM

Variable	Description	Value used in temperature equation	Min	Max	Units	Error in calculation of ΔT (ΔELA = −980 m)	Reference
r [a]	resistance to sensible and latent heat transfer	56	47	70	s/m	±0.2°C	Kaser and Osmaston (2002)
$\delta P/\delta z$	precipitation gradient	-3.225×10^{-3}	-1.360×10^{-3}	-5.090×10^{-3}	kg m^{-2} m^{-1} day^{-1}	±0.5°C	Pulwarty (1998)
ΔP	change in precipitation	0	−500	500	kg m^{-2}	±0.4°C	–
ΔELA	change in ELA	−980	−880	−1080	m	±0.9°C	this study
$\delta t/\delta z$	lapse rate	0.65	0.55	0.75	°C/100 m	±1.0°C	–
δpva/δz	atmospheric absolute humidity gradient	-1.223×10^{-6}	-1.55×10^{-6}	-8.94×10^{-6}	kg m^{-3} m^{-1}	±0.9°C	NCEP
					Combined effect of errors on ΔT	±1.8°C	

[a] Used to calculate transfer coefficients for sensible and latent heat transfer.

https://doi.org/10.1016/j.yqres.2006.07.005 Published online by Cambridge University Press

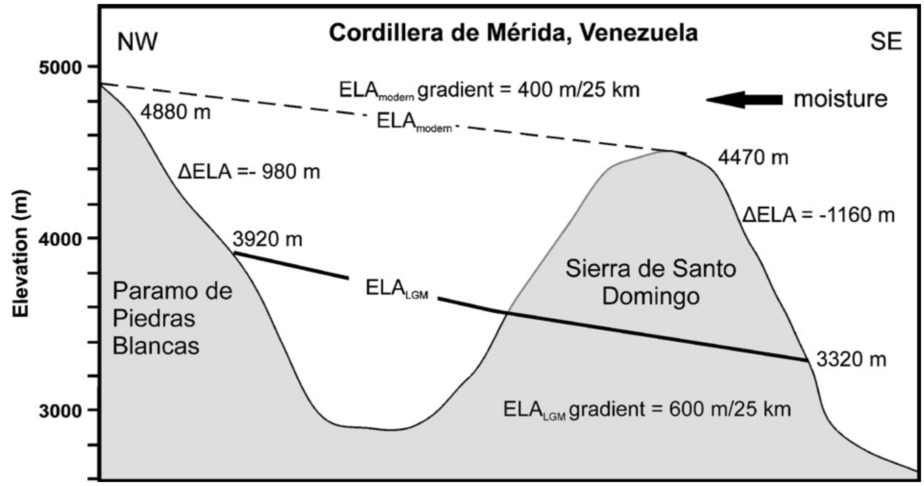

Figure 4. Graphical representation of the LGM versus modern ELA values. ΔELA values indicate the difference between modern and LGM ELA values within individual regions. ΔELA values are a result of temperature change. The distribution of ELAs across different slopes is controlled by precipitation patterns and cloudiness that are restricted on NW slopes. The data presented here tentatively suggest that the gradient of ELA values during the LGM was slightly steeper than today.

greatest variability (±1.0°C). The combined error for the estimated temperature lowering is ±2°C, determined from the square root of the sum of squared errors.

Discussion

LGM paleo-temperature estimates

An ELA lowering is commonly converted to temperature change by multiplying an average atmospheric lapse rate by the ΔELA (e.g. Porter, 2001). This method is useful as an estimate of paleo-temperatures in regions where modern meteorological data are not available. However, this technique has limitations because thermodynamic processes on glacial surfaces are complex and the ELA responds to more than just changes in atmospheric temperature. As an alternative to lapse rate calculations, combined energy and mass-balance modeling of the ELA (Kuhn, 1989) can provide better estimates of the climate associated with an ELA change. The Kuhn (1989) equation is limited because it can only be used in regions where precipitation is abundant; however, it is advantageous over a lapse rate calculation because it recognizes that the rates of latent and sensible heat loss, humidity, and precipitation change with elevation. If these additional gradients are not considered, the temperature change associated with an ELA lowering is simplified to the atmospheric lapse rate calculation. The Kuhn (1989) equation assumes that the temperature of the ice surface at the ELA is 0°C, which is not necessarily fixed to the atmospheric 0°C isotherm (Ohmura et al., 1992). This is a reasonable hypothesis where precipitation is abundant and melting is the dominant source of ablation (Seltzer, 1992). Conditions were probably drier in Venezuela during the LGM than today but it is assumed that precipitation was abundant enough to maintain mass-balance processes that are similar to the modern system.

The paleo-temperature estimates presented in this paper are with respect to the northern Sierra de Santo Domingo, where precipitation is abundant and modern glaciers exist for comparison. Using a ΔELA estimate of −980 m, the Kuhn equation requires a temperature reduction of 8.8±2°C for the Mérida Andes during the LGM. The −980 m ΔELA is in reference to a modern ELA estimated from glaciers that are not in equilibrium with the modern climate. Therefore, compared to today's freezing height, it is possible that the true ΔELA is closer to −1200 m, which requires a temperature reduction of 11.0± 2°C. Nevertheless, even the minimum temperature change estimates presented here are greater than what would be estimated using an atmospheric lapse rate calculation (−6.4± 1.0°C). Seltzer (1992) used the same equation to calculate a paleo-temperature change in the Cordillera Real, Bolivia, and also found that an atmospheric lapse rate calculation underestimated the cooling associated with an ELA lowering in that region.

Glacier variability in the tropics is driven by changes in temperature, precipitation, solar radiation or a combination thereof. Precipitation did not likely account for the observed lowering of ELA values for the northern Andes during the LGM because paleoenvironmental records indicate that the region was drier than today (Bradbury et al., 1981; Bradley et al., 1985; Weingarten et al., 1991; Salgado-Labouriau et al., 1992). Likewise, changes in potential radiation at the top of the atmosphere were not a major contributor, because northern hemisphere insolation values during the LGM were similar to today (Berger, 1978). The results presented here suggest that temperature change was the principal cause of glacier surface-area changes in the Venezuelan Andes during the LGM. Although albedo changes are the dominant control of mass-balance fluctuations for modern tropical glaciers (e.g. Favier et al., 2004), albedo changes are closely related to temperature, precipitation and humidity. Decreasing temperatures would lower the freezing height, increase the available accumulation area and increase the relative amount of frozen (high-albedo) precipitation on a glacier's surface. Assuming the glacier mass-balance processes that operated during the LGM were similar to today, an increased accumulation area would require an increased ablation area to balance the additional volume of

https://doi.org/10.1016/j.yqres.2006.07.005 Published online by Cambridge University Press

ice. Thus, lower temperatures would increase glacial coverage and ELAs would be at lower elevations. This supports Seltzer's (1992) conclusion that in humid regions, temperature plays a larger role than precipitation in driving ELA variability.

LGM ELA gradient

Temperature change is the primary cause of late Quaternary ELA variability within an individual valley in the Venezuelan Andes. However , the gradient in ELA values across the region are driven more by local conditions, such as precipitation, cloud cover and aspect. The ELA estimates from the three regions in the Cordillera de Mérida suggest that there was an ELA gradient of ~600 m per 25 km during the LGM (Fig. 4). The lowest ELA values were in the southeast and the highest were in the northwest. The results from this study are similar to the asymmetric elevations of mapped cirque floors that Schubert (1987) concluded was a response to precipitation patterns during the LGM. Using Eq. (2), the modern ELA gradient would be ~400 m per 25 km. This is a first estimate and needs to be evaluated cautiously; however, it suggests that the LGM gradient was steeper than today. A steeper ELA gradient in the Andes may have been the result of drier conditions during the LGM (Klein et al., 1999). Alternatively, the ELA gradient may have been driven by a steeper precipitation gradient with a greater increase on southeastern than northwestern slopes, but this seems unlikely given the strong evidence for drier local LGM conditions. It should also be considered that the modern ELA gradient may be steeper than indicated by Eq. (2), possibly as a result of differences in cloudiness alone, which are not considered in this equation. The direction of the LGM and modern ELA gradients are similar, which suggests that wind direction and the primary moisture source were the same.

The regional precipitation patterns likely explain the ELA gradient between the northern and southern Santo Domingo slopes but not the ELAs in the Paramo de Piedras Blancas. Modern precipitation differs by up to 800 mm/yr for the northern and southern Santo Domingo slopes, whereas the precipitation difference is minimal between the Santo Domingo and the Paramo de Piedras Blancas (~100 mm/yr). Greater cloud cover in the Santo Domingo region compared to the Paramo de Piedras Blancas, combined with less precipitation in the Piedras Blancas region, may account for the differences in ELA values. The diurnal pattern of cloudiness and solar azimuth play a substantial role in regional glacial variability in the tropics by decreasing the amount of effective radiation received by the ice surface (e.g. Hastenrath, 1985; Mölg et al., 2003). Cloudiness is especially pronounced during the rainy season in the Santo Domingo region (Azocar and Monasterio, 1980) where substantial cloud cover is a common feature during the late morning and early afternoon. In contrast, cloud cover in the Piedras Blancas region is greatly reduced.

Comparison to previous reports

In this section, the results from the Venezuelan Andes are compared to published estimates of ELA changes during the LGM in tropical South and Central America. It is important to recognize that the ability to compare results from different regions is limited by the variety of methods used to estimate ΔELAs. For example, many ΔELAs are calculated relative to the modern 0°C isotherm instead of a modern ELA, and the same calculations were applied to the data presented in this report for comparison purposes. If the ΔELA estimates in this paper are referenced to today's freezing height of 4860 m, rather than modern glacier ELAs, ΔELAs may have been as great as −1030 to −1420 m. This type of ΔELA estimate should be viewed with caution because the modern 0°C isotherm is difficult to determine, is not always in equilibrium with existing glacier and does not necessarily correspond with the ELA.

The calculated LGM ELA lowerings in this paper are comparable to other reports from the Venezuelan Andes (Fig. 5). Northwest of the Paramo de Piedras Blancas and the Sierra de Santo Domingo is the Paramo de La Culata, where Schubert and Valastro (1974) reported that ELAs were ~1200 m lower than today. This change in ELA was estimated based on LGM cirque floor elevations of 3500 m relative to a modern 4700-m 0°C isotherm. Porter (2001) estimated an LGM ELA lowering of ~900 m for the Venezuelan Andes using the median-altitude method and a 4700-m 0°C isotherm. This should be viewed as a minimal estimate because the median-altitude method calculates an ELA based on the elevation half-way between a glacier's headwall and terminus (Porter, 2001). Porter's estimate likely underestimates the ELA lowering for Venezuela because the true ELA is situated at a lower elevation than the mid-point of a glacier (Kaser and Osmaston, 2002).

The median altitude method was also used to calculate a 1075 m lower ELA in Colombia referenced to today's 0°C

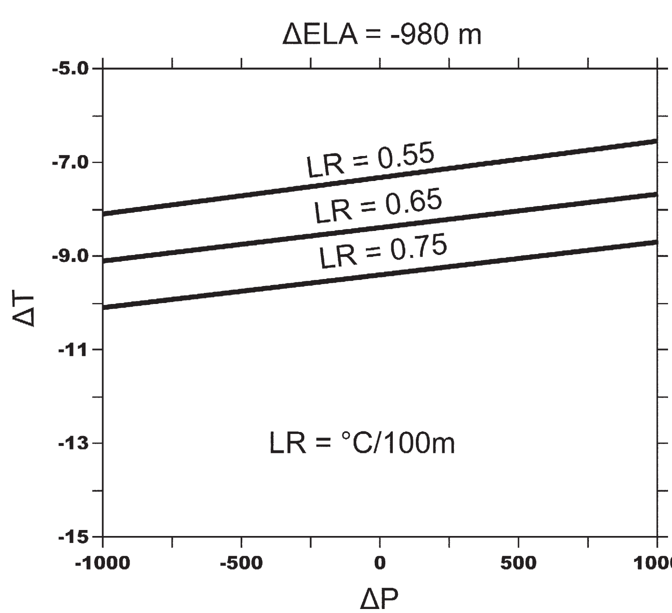

Figure 5. Graphical representation of LGM equilibrium-line altitude lowerings in the Venezuelan Andes, and the effects of changes in precipitation and atmospheric lapse rate (LR) values on the estimated temperature lowerings.

https://doi.org/10.1016/j.yqres.2006.07.005 Published online by Cambridge University Press

isotherm (Hoyos-Patiño, 1998; Porter, 2001). The toe-to-headwall ratio (THAR) method is a modification of the median altitude method which more closely approximates the ELA because a ratio other than 0.5 can be used (Meirding, 1982). ELAs of up to 1500 m lower were reported for Costa Rica using today's 0°C isotherm combined with the AAR and THAR methods (Lachniet and Seltzer, 2002). ELA lowerings between ~550 and 1200 m were calculated for the Central Andes using the THAR and cirque-floor elevation methods (Klein et al., 1999), and up to 920 m in Ecuador using the median-altitude method (Clapperton, 1987, 1993; Porter, 2001). To summarize, some of the older published ELA values for the tropics rely on approximate methods, such as the median-altitude method, and these reports may underestimate the amount of tropical LGM ELA lowering. The THAR, AAR and AABR methods are more accurate reconstruction techniques and commonly yield greater ΔELA values.

The temperature estimates based on ELA reconstructions presented here are supported by independent lines of evidence that indicate a large cooling at high elevations in the northern tropics during the LGM. Rull (1998) estimated a temperature lowering of 7±1°C for the LGM in the Venezuelan Andes based on a ~1200-m descent of vegetation zones relative to today, and an atmospheric lapse rate calculation. Lachniet and Seltzer (2002) estimate a LGM cooling of 8 to 9°C for Costa Rica based on an atmospheric lapse rate calculation. Furthermore, Mark et al. (2005) concluded that the greatest tropical LGM ELA lowering occurred in the northern Andes, Mexico and Papua New Guinea. The paleo-temperature results for the northern tropics summarized here are greater than vegetation, lake-level and geochemical studies that indicate temperatures at high Andean elevations were ~5 to 6.4°C cooler during the LGM (Farrera et al., 1999). Interestingly, ice-core evidence from the Peruvian Andes indicates high elevation temperatures may have been as much as 8 to 12°C cooler than modern (Thompson et al., 1995), though an alternative interpretation of the $\delta^{18}O$ from the Huascaran ice cores suggests that this may be an overestimate (Pierrehumbert, 1999).

Discrepancy between low and high elevation paleo-temperature reconstructions

The large cooling at high elevations inferred from glacial ELAs for the northern hemisphere tropics does not directly correspond to reconstructed changes in temperature at the ocean surface. For example, the maximum estimated tropical Atlantic temperatures were only 5 to 6°C cooler during the LGM (Guilderson et al., 1994; Thompson et al., 1995; Stute et al., 1995; Mix et al., 1999). Paleo-temperature estimates from the Cariaco Basin, off the north coast of Venezuela, indicate conditions were ~3 to 4°C cooler during the LGM (Lin et al., 1997; Lea et al., 2003). This leaves at least a ~3°C and up to ~5°C discrepancy between the temperature reconstructions proposed for sea-surface and the high-elevation temperature reconstructions presented in this paper.

The discrepancy between sea-surface and high-elevation paleo-temperature estimates is an area of active research. One explanation is that a steeper atmospheric lapse rate would lower the freezing height relative to sea surface. This is controversial because it is difficult to find an adequate mechanism capable of producing such steep values (Rind and Peteet, 1985). Betts and Ridgeway (1992) suggested that another mechanism is required to lower the freezing height, such as a reduction of mean surface wind speed, or an increase in the net atmospheric transport of tropical heat. Using the model of Betts and Ridgeway (1989), Greene et al. (2002) showed that the observed LGM tropical ELA lowering can be achieved with an average tropical SST cooling of only 2.8°C and a reduction in the equivalent potential temperature of the atmospheric mixing layer. To summarize, climate modeling studies suggest that temperature changes at high elevations during the LGM were not necessarily equal to those at sea surface. In fact, a more comprehensive evaluation of glacio-geological evidence from certain regions indicates that there may be an even greater discrepancy between LGM temperature values at sea surface and high elevations than previously proposed.

Conclusions

ELAs were 850 to 1420 m lower than present in the Venezuelan Andes during the LGM. This supports the contention of Mark et al. (2005) that ELA values during the LGM were lower in the northern Andes than the central Andes. The associated temperatures were lower in the Venezuelan Andes during the LGM by at least 8.8±2.0°C and possibly as much as 11°C using a combined energy and mass-balance equation. This is ~2°C cooler than the value estimated by an atmospheric lapse rate calculation. The values for the northern tropics are greater than the overall tropical average for LGM cooling of 5° to 6.4°C previously presented and calculated with the atmospheric lapse rate (Porter, 2001). Lapse rate calculations underestimate the cooling associated with lower ELA values because they do not take into account the energy budget across a glacier's surface and neglect the controls of the altitude gradients of humidity and precipitation on the ELA. There is a discrepancy between low- and high-altitude paleo-temperature estimates during the LGM for the northern tropics and an adequate explanation needs to be proposed with future modeling studies. The spatial gradient of LGM ELA values in Venezuela is consistent with the modern cloudiness and precipitation patterns, suggesting that similar patterns were present during the LGM. There is tentative evidence of a steeper ELA gradient during the LGM that could have been the result of a drier atmosphere.

Acknowledgments

The authors would like to thank Matthew Lachniet and Henry Osmaston for materials that helped with the methods section of this paper. Maximiliano Bezada provided field and logistical support. Michael Ramsey, Thomas Anderson and two anonymous reviewers provided valuable comments that improved an earlier version of the manuscript. This project was supported by NSF grant ATM-9809472.

References

Ames, A., Francou, B., 1995. Cordillera Blanca, Glaciares en la Historia. Bulletin de l'Institut Francais d'Etudes Andines 24, 37–64.

Azocar, A., Monasterio, M., 1980. Caracterización Ecológica del Clima en El Páramo de Mucubají. In: Monasterio, M. (Ed.), Estudios Ecologicos en los Páramos Andinos. Ediciones de la Universidad de Los Andes, Merida, Venezuela, pp. 207–223.

Benn, D., I., Evans, D.J.A., 1998. Glaciers and Glaciation. John Wiley and Sons, Inc., New York.

Berger, A.L., 1978. Long-term variations of caloric insolation resulting from the Earth's orbital elements. Quaternary Research 9, 139–167.

Betts, A.K., Ridgeway, W., 1989. Climate equilibrium of the atmospheric convective boundary layer over a tropical ocean. Journal of the Atmospheric Sciences 46, 2621–2641.

Betts, A.K., Ridgeway, W., 1992. Tropical boundary layer equilibrium in the Last Ice Age. Journal of Geophysical Research 97, 2529–2534.

Bradbury, J.P., Leyden, B., Salgado-Labouriau, M., Lewis Jr., W.M., Schubert, C., Binford, M.W., Frey, D.G., Whitehead, D.R., Weibezahn, F.H., 1981. Late quaternary environmental history of Lake Valencia, Venezuela. Science 214, 1299–1305.

Bradley, R.S., Yuretich, R., Salgado-Labouriau, M.L., Weingarten, B., 1985. Late Quaternary paleoenvironmental reconstruction using lake sediments from the Venezuelan Andes: preliminary results. Zeitschrift für Gletscherkunde und Glazialgeologie 21, 97–106.

Bradley, R., Yuretich, R., Weingarten, B., 1991. Studies of modern climate. In: Yuretich, R. (Ed.), Late Quaternary Climatic Fluctuations of the Venezuelan Andes. University of Massachusetts, Amherst, MA, pp. 45–62.

Broecker, W.S., 1997. Mountain glaciers: recorders of atmospheric water vapor content? Global Biogeochemical Cycles 11, 589–597.

Clapperton, C.M., 1987. Glacial geomorphology, Quaternary glacial sequence and palaeoclimatic inferences in the Ecuadorian Andes. In: Gardiner, V. (Ed.), International Geomorphology 1986, Part II. Wiley, Chichester, pp. 843–870.

Clapperton, C.M., 1993. Quaternary Geology and Geomorphology of South America. Elsevier, Amsterdam.

CLIMAP, P.M., 1976. The surface of the ice-age earth. Science 191, 1131–1137.

CLIMAP, P.M., 1981. Seasonal reconstruction of the earth's surface at the last glacial maximum. Geological Society of America Map and Chart Series.

Denton, G.H., Heusser, C.J., Lowell, T.V., Schluchter, C., Andersen, B.G., Heusser, L.E., Moreno, P.I., Marchant, D.R., 1999. Geomorphology, Stratigraphy, and Radiocarbon Chronology of Llanquihue Drift in the Area of the Southern Lake District, Seno Reloncavi, and Isla Grande de Chiloe, Chile. Geografiska Annaler 81A, 167–229.

Fairbanks, R.G., 1989. A 17,000-year glacio-eustatic sea level record: influence of glacial melting rates on the Younger Dryas event and deep-ocean circulation. Nature 342, 637–642.

Farrera, I., Harrison, S.P., Prentice, I.C., Ramstein, G., Guiot, J., Bartlein, P.J., Bonnefille, R., Bush, M., Cramer, W., von Grafenstein, U., Holmgren, K., Hopogheimstra, H., Hope, G., Jolly, D., Lauritzen, S.-E., Ono, Y., Pinot, S., Stute, M., Yu, G., 1999. Tropical climates at the last glacial maximum: a new synthesis of terrestrial palaeoclimate data: I. Vegetation, lake-levels and geochemistry. Climate Dynamics 15, 823–856.

Favier, V., Wagnon, P., Ribstein, 2004. Glaciers of the outer and inner tropics: a different behaviour but a common response to climatic forcing. Geophysical Research Letters 31, L16403, doi:10.1029/2004GL020654.

Francou, B., Ribstein, P., Saravia, R., Tiriau, E., 1995. Monthly balance and water discharge of an inter-tropical glacier: Zongo Glacier, Cordillera Real, Bolivia, 16°S. Journal of Glaciology 41, 61–67.

Furbish, D.J., Andrews, J.T., 1984. The use of hypsometry to indicate long-term stability and response of valley glaciers to changes in mass transfer. Journal of Glaciology 30, 199–211.

Giegengack, R., Grauch, R., 1973. Quaternary geology of the central Andes, Venezuela: a preliminary assessment. Excursion 1, 38–93.

Greene, A.M., Seager, R., Broecker, W.S., 2002. Tropical snowline depression at the last glacial maximum: comparison with proxy records using a single-cell tropical climate model. Journal of Geophysical Research 107 (ACL 4-1 to 17.).

Guilderson, T.P., Fairbanks, R.G., Rubenstone, J.L., 1994. Tropical temperature variations since 20,000 years ago: modulating interhemispheric climate change. Science 263, 663–665.

Hastenrath, S., 1984. Interannual variability and the annual cycle: mechanisms of circulation and climate in the tropical Atlantic sector. Monthly Weather Review 112, 1097–1107.

Hastenrath, S., 1985. Climate and ciculation of the tropics. C. Reidel Publishing Company, Dordrecht.

Hastenrath, S., 1989. Ice flow and mass changes of Lewis Glacier, Mount Kenya, East Africa: observations 1974–86, modeling, and predictions to the year 2000 A.D. Journal of Glaciology 35, 325–332.

Hoyos-Patiño, F., 1998. Glaciers of colombia. In: Williams, Ferrigno, J.G. (Eds.), Glaciers of South America, Satellite Image Atlas of Glaciers of the World. U.S. Geological Survey Professional Paper 1386-I, pp. 111–130.

Jordan, E., 1991. Die Gletscher der bolivianischen Andean. Franz Steiner Verlag Stuttgart, Eurasburg, Germany.

Kalnay, E., co-authors, 1996. The NCEP/NCAR reanalysis 40-year project. Bulletin of the American Meteorological Society 77, 437–471.

Kaser, G., 1995. Some notes on the behavior of tropical glaciers. Bulletin de l'Institut Francais d'Etudes Andines 24, 671–681.

Kaser, G., 2001. Glacier–climate interaction at low latitudes. Journal of Glaciology 47, 195–204.

Kaser, G., Georges, C., 1999. On the mass balance of low latitude glaciers with particular consideration of the Peruvian Cordillera Blanca. Geografiska Annaler 81A, 643–651.

Kaser, G., Noggler, B., 1996. Glacier fluctuations in the Ruwenzori Range (East Afrika) during the 20th century. A preliminary report. Zeitschrift Gletscherkunde Glazialgeologie 32, 109–117.

Kaser, G., Osmaston, H., 2002. Tropical Glaciers. Cambridge University Press, Cambridge.

Klein, A.G., Seltzer, G.O., Isacks, B.L., 1999. Modern and last local glacial maximum snowlines in the Central Andes of Peru, Bolivia, and Northern Chile. Quaternary Science Reviews 18, 63–84.

Kuhn, M., 1989. The response of the equilibrium line altitude to climate fluctuations: theory and observations. In: Oerlemans, J. (Ed.), Glacier Fluctuations and Climate Change. Kluwer Academic Publishers, The Netherlands, pp. 407–417.

Lachniet, M.S., Seltzer, G., 2002. Late Quaternary glaciation of Costa Rica. GSA Bulletin 114, 547–558.

Lea, D.W., Pak, D.K., Peterson, L.C., Hughen, K.A., 2003. Synchronicity of tropical and high-latitude Atlantic temperatures over the last glacial termination. Science 301, 1361–1364.

Lin, H.-L., Peterson, L.C., Overpeck, J.T., Trumbore, S.E., Murray, D.W., 1997. Late Quaternary climate change from $\delta^{18}O$ records of multiple species of planktonic foraminifera: high-resolution records from the anoxic Cariaco Basin, Venezuela. Paleoceanography 12, 415–427.

Lowell, T.V., Heusser, C.J., Andersen, B.G., Moreno, P.I., Hauser, A., Heusser, L.E., Schluchter, C., Marchant, D.R., Denton, G.H., 1995. Interhemispheric correlation of late pleistocene glacial events. Science 269, 1541–1549.

Mahaney, W.C., Milner, M.W., Voros, J., Kalm, V., Hutt, G., Bezada, M., Hancock, R.G.V., Aufreiter, S., 2000. Stratotype for the Mérida Glaciation at Pueblo Llano in the northern Venezuelan Andes. Journal of South American Earth Sciences 13, 761–774.

Mann, D.H., Hamilton, T.D., 1995. Late pleistocene and holocene paleoenvironments of the north Pacific coast. Quaternary Science Reviews 14, 449–471.

Mark, B.G., Harrison, S., Spessa, A., New, M., Evans, D.J.A., Helmens, K.F., 2005. Tropical snowline changes at the last glacial maximum: a global assessment. Quaternary International 138–139, 168–201.

Meirding, T.C., 1982. Late pleistocene glacial equilibrium-line altitudes in the Colorado front range: a comparison of methods. Quaternary Research 18, 289–310.

Mix, A.C., Morey, A.E., Pisias, N.G., Hostetler, S.W., 1999. Foraminifera faunal estimates of paleotemperature: circumventing the no-analog problem yields cool ice age tropics. Paleoceanography 14, 350–359.

Mölg, T., Georges, C., Kaser, G., 2003. The contribution of increased incoming shortwave radiation to the retreat of the Rwenzori Glaciers, East Africa, during the 20th century. International Journal of Climatology 23, 291–303.

Monasterio, M., 1986. Adaptive Strategies of Espeletia in the Andean Desert Paramo. Oxford University Press, London.

Monasterio, M., Reyes, S., 1980. Diversidad ambiental y variacion de la vegetacion en los páramos de los Andes Venezolanos. In: Monasterio, M. (Ed.), Estudios Ecologicos en los Páramos Andinos. Ediciones de la Universidad de Los Andes, Merida, Venezuela, pp. 47–91.

Oerlemans, J., 2001. Glaciers and Climate Change. A.A. Balkema Publishers, Amsterdam.

Ohmura, A., Kasser, P., Funk, M., 1992. Climate at the equilibrium line of glaciers. Journal of Glaciology 38, 397–411.

Osmaston, H., 2005. Estimates of glacier equilibrium line altitudes by the Area × Altitude, the Area × Altitude Balance Ratio and the Area × Altitude Balance Index methods and their validation. Quaternary International 138–139, 22–31.

Osmaston, H., 2006. Should quaternary sea-level changes be used to correct glacier ELAs, vegetation belt altitudes and sea level temperatures for inferring climate changes. Quaternary Research 65, 244–251.

Paterson, W.S.B., 1981. The Physics of Glaciers. Pergamon Press Inc., New York.

Pierrehumbert, R.T., 1999. Huascaran δ^{18}O as an indicator of tropical climate during the last glacial maximum. Geophysical Research Letters 26, 1345–1348.

Polissar, P.J., 2005. Unpublished PhD. Dissertation. University of Massachusetts at Amherst.

Porter, S.C., 2001. Snowline depression in the tropics during the Last Glaciation. Quaternary Science Reviews 20, 1067–1091.

Pulwarty, R.S., Barry, R.G., Hurst, C.M., Sellinger, K., Mogollon, L.F., 1998. Precipitation in the Venezuelan Andes in the context of regional climate. Meteorology and Atmospheric Physics 67, 217–237.

Rind, D., Peteet, D., 1985. Terrestrial conditions at the Last Glacial Maximum and CLIMAP sea-surface temperature estimates: are they consistent? Quaternary Research 24, 1–22.

Rull, V., 1998. Palaeoecology of pleniglacial sediments from the Venezuelan Andes. palynological record of El Caballo stadial, sedimentation rates and glacier retreat. Review of Palaeobotany and Palynology 99, 95–114.

Salgado-Labouriau, M.L., 1979. Modern pollen deposition in the Venezuelan Andes. Grana 18, 53–68.

Salgado-Labouriau, M.L., Bradley, R.S., Yuretich, R., Weingarten, B., 1992. Paleoecological analysis of the sediments of Lake Mucubaji, Venezuelan Andes. Journal of Biogeography 19, 317–327.

Schubert, C., 1970. Glaciation of the Sierra de Santo Domingo, Venezuelan Andes. Quaternaria 13, 225–246.

Schubert, C., 1972. Geomorphology and glacier retreat in the Pico Bolivar area, Sierra Nevada de Merida, Venezuela. Zeitschrift für Gletscherkunde und Glazialgeologie VIII, 189–202.

Schubert, C., 1974. Late Pleistocene Mérida Glaciation, Venezuelan Andes. Boreas 3, 147–151.

Schubert, C., 1987. La Extension de los Glaciares Pleistocenes en la Sierra Nevada de Merida. Boletín de la Sociedad Venezolana de Ciencias Naturales 41, 299–308.

Schubert, C., 1984. The Pleistocene and recent extent of the glaciers of the Sierra Nevada de Merida, Venezuela. Erdwissenschaftliche Forschung 18, 269–278.

Schubert, C., 1992. The glaciers of the Sierra Nevada de Merida (Venezuela): a photographic comparison of recent deglaciation. Erdkunde 46, 58–64.

Schubert, C., 1998. Glaciers of Venezuela. Glaciers of South America. USGS Professional Paper 1386-I.

Schubert, C., Clapperton, C., 1990. Quaternary Glaciations in the Northern Andes (Venezuela, Colombia and Ecuador). Quaternary Science Reviews 9, 123–135.

Schubert, C., Rinaldi, M., 1987. Nuevos Datos Sobre la Cronologia del Estadio Tardio de la Glaciacion Merida, Andes Venezolanos. Acta Cientifica 38.

Schubert, C., Valastro, S., 1974. Late Pleistsocene glaciation of Paramo de La Culata, north-central Venzuelan Andes. Sonderdruck aus der Geologischen Rundschau 63, 517–537.

Seltzer, G.O., 1992. Late Quaternary glaciation of the Cordillera Real, Bolivia. Journal of Quaternary Science 7, 87–98.

Seltzer, G.O., 1994. A lacustrine record of late pleistocene climatic change in the subtropical Andes. Boreas 23, 105–111.

Seltzer, G., Rodbell, D.T., Baker, P.A., Fritz, S., Tapia, P.M., Rowe, H.D., Dunbar, R.B., 2002. Early warming of tropical South America at the last glacial–interglacial transition. Science 296, 1685–1686.

Smith, J.A., Seltzer, G.O., Farber, D.L., Rodbell, D.T., Finkel, R.C., 2005. Early local last glacial maximum in the tropical Andes. Science 308, 678–681.

Stute, M., Forster, M., Frischkorn, H., Serejo, A., Clark, J.F., Schlosser, P., Broecker, W.S., Bonani, G., 1995. Cooling of Tropical Brazil (5°C) during the last glacial maximum. Science 269, 379–383.

Thompson, L.G., Mosley-Thompson, E., Davis, M.E., Lin, P.-N., Henderson, K.A., Cole-Dai, J., Bolzan, J.F., Liu, K.-b., 1995. Late glacial stage and holocene tropical ice core records from Huascarán, Peru. Science 269, 46–50.

Weingarten, B., Salgado-Labouriau, M.L., Yuretich, R., Bradley, R., 1991. Late quaternary environmental history of the Venezuelan Andes. In: Yuretich, R. (Ed.), Late Quaternary Climatic Fluctuations of the Venezuelan Andes. University of Massachusetts, Amherst, MA, pp. 63–94.

https://doi.org/10.1016/j.yqres.2006.07.005 Published online by Cambridge University Press